

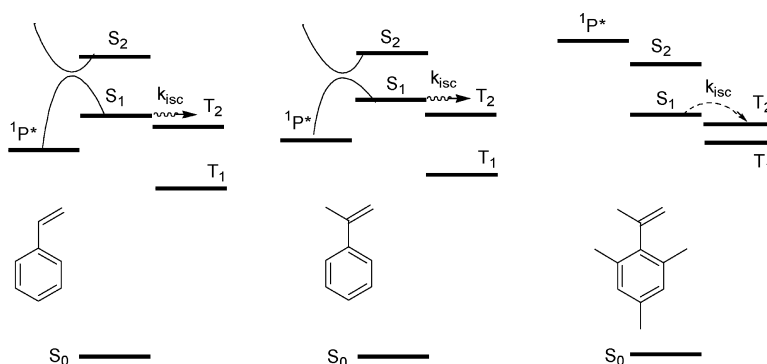
Article

Activated Decay Pathways for Planar vs Twisted Singlet Phenylalkenes

Frederick D. Lewis, and Xiaobing Zuo

J. Am. Chem. Soc., **2003**, 125 (29), 8806-8813 • DOI: 10.1021/ja035066j • Publication Date (Web): 24 June 2003

Downloaded from <http://pubs.acs.org> on March 29, 2009



More About This Article

Additional resources and features associated with this article are available within the HTML version:

- Supporting Information
- Links to the 1 articles that cite this article, as of the time of this article download
- Access to high resolution figures
- Links to articles and content related to this article
- Copyright permission to reproduce figures and/or text from this article

[View the Full Text HTML](#)

Activated Decay Pathways for Planar vs Twisted Singlet Phenylalkenes

Frederick D. Lewis* and Xiaobing Zuo

Contribution from the Department of Chemistry, Northwestern University,
Evanston, Illinois 60208-3113

Received March 9, 2003; E-mail: lewis@chem.northwestern.edu

Abstract: The ground state conformation, spectroscopy, and photochemical behavior of styrene and eight of its vinyl- and ring-methylated derivatives have been investigated. Introduction of methyl groups at the α -position of the vinyl group or the ortho positions of the phenyl results in increased phenyl–vinyl dihedral angles. Styrenes possessing both α -methyl and ortho-methyl groups adopt orthogonal geometries. Decreased planarity results in a progressive blue-shift in the lowest energy allowed π, π^* transition and a decrease in the singlet lifetime. Kinetic modeling of the temperature-dependent singlet lifetimes provides activation parameters for the activated decay pathway, which is assigned to C=C torsion for styrenes with phenyl–vinyl dihedral angles, ϕ , $< 60^\circ$. Planar styrenes have large torsional barriers (7 ± 1 kcal/mol) and decay predominantly via intersystem crossing and fluorescence at room temperature. Styrenes with values of $30^\circ < \phi < 60^\circ$ have smaller torsional barriers and decay predominantly via C=C torsion at room temperature. Highly nonplanar styrenes decay predominantly via relatively rapid, weakly activated intersystem crossing.

Introduction

The excited singlet states of styrene have been investigated with a wide variety of experimental and theoretical methods.^{1–5} Both gas phase spectroscopy and theory indicate that the lowest singlet state of styrene, like its ground state, is essentially planar and has a large barrier (>4 kcal/mol) to C=C torsion. The styrene torsional barrier has not been measured, but has been the subject of several recent calculations, which provide values in excess of 14 kcal/mol.^{3,4} These values are sufficiently high to effectively preclude isomerization on the singlet surface. Nearly a decade ago, we investigated the temperature-dependence of the singlet lifetimes and isomerization quantum yields for *trans*- and *cis*-1-phenylpropene.^{6,7} Standard Arrhenius treatment of these data, after correction of the isomerization data for temperature-independent intersystem crossing, provided activation energies of 8.8 and 4.6 kcal/mol for the *trans* and *cis* isomers, respectively. Because the β -methyl substituents of the 1-phenylpropenes might be expected to stabilize the twisted

intermediate formed from C=C torsion, it seemed likely that the barrier for styrene might be higher than that for *trans*-1-phenylpropene.

The absence of geometric isomers for styrene precludes investigation of its singlet torsional barrier by the direct method used for the 1-phenylpropenes. However, if C=C torsion is the only activated singlet state decay process, the barrier can be obtained simply from nonlinear fitting of the singlet decay time using eq 1

$$\tau(T) = I/[\Sigma k + A \exp(-E_a/RT)] \quad (1)$$

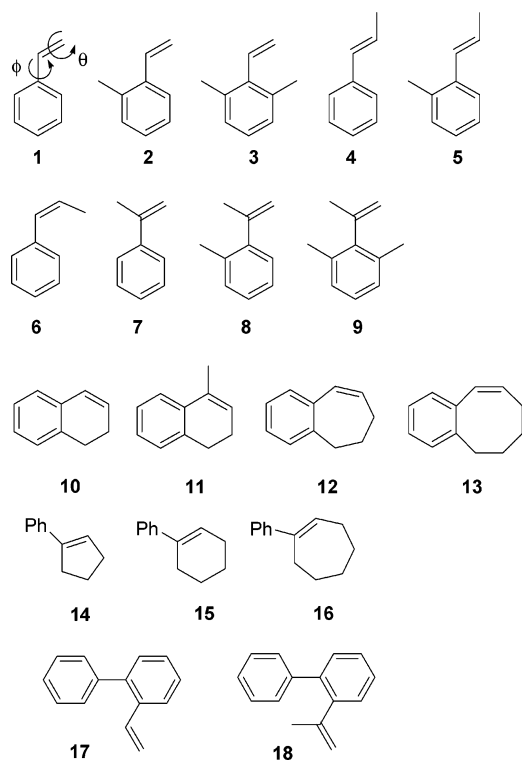
where Σk is the sum of all nonactivated processes (fluorescence and intersystem crossing), and A and E_a are the preexponential and activation energy, respectively, for the activated process. Nonlinear fitting of temperature-dependent singlet lifetimes has been successfully employed in our studies of the di- π -methane rearrangement of 1,3-diphenylpropenes⁸ and the conformer-specific photoisomerization of 2-vinylbiphenyls.^{9,10} In addition, nonlinear fitting of our lifetime data for the 1-phenylpropenes provides activation parameters similar to those obtained previously using both quantum yield and lifetime data.

We report here the results of an investigation of the absorption and fluorescence spectra and singlet lifetimes of styrene (**1**), eight methylated derivatives (**2–9**), and two cyclic analogues (**10** and **11**) whose structures are shown in Chart 1.¹¹ The

- (1) (a) Hui, M. H.; Rice, S. A. *J. Chem. Phys.* **1974**, *61*, 833–842. (b) Crosby, P. M.; Salisbury, K. *J. Chem. Soc. Chem. Commun.* **1975**, 477–478. (c) Syage, J. A.; Adel, F. A.; Zewail, A. H. *Chem. Phys. Lett.* **1983**, *103*, 15–22. (d) Haas, Y.; Kendler, S.; Zingher, E.; Zuckermann, H.; Zilberg, S. *J. Chem. Phys.* **1995**, *103*, 37–47. (e) Zilberg, S.; Haas, Y. *J. Chem. Phys.* **1995**, *103*, 20–35.
- (2) Condirston, D. A.; Laposa, J. D. *Chem. Phys. Lett.* **1979**, *63*, 313–317.
- (3) Bearpark, M. J.; Olivucci, M.; Wilsey, S.; Bernardi, F.; Robb, M. A. *J. Am. Chem. Soc.* **1995**, *117*, 6944–6953.
- (4) (a) Bearpark, M. J.; Bernardi, F.; Olivucci, M.; Robb, M. A. *J. Phys. Chem. A* **1997**, *101*, 8395–8401. (b) Molina, V.; Merchán, M.; Roos, B. O.; Malmqvist, P.-A. *Phys. Chem. Chem. Phys.* **2000**, *2*, 2211–2217.
- (5) (a) Amatatsu, Y. *Chem. Phys. Lett.* **2001**, *344*, 200–206. (b) Amatatsu, Y. *J. Comput. Chem.* **2002**, *23*, 950–956. (c) Amatatsu, Y. *J. Comput. Chem.* **2002**, *23*, 928–937.
- (6) Lewis, F. D.; Bassani, D. M. *J. Am. Chem. Soc.* **1993**, *115*, 7523–7524.
- (7) Lewis, F. D.; Bassani, D. M.; Caldwell, R. A.; Unnett, D. J. *J. Am. Chem. Soc.* **1994**, *116*, 10 477–10 485.

- (8) Lewis, F. D.; Zuo, X.; Kalgutkar, R. S.; Wagner-Brennan, J. M.; Miranda, M. A.; Font-Sanchis, E.; Perez-Prieto, J. *J. Am. Chem. Soc.* **2001**, *123*, 11 883–11 889.
- (9) Lewis, F. D.; Zuo, X.; Gregvoryan, V.; Rubin, M. *J. Am. Chem. Soc.* **2002**, *124*, 13 664–13 665.
- (10) Lewis, F. D.; Zuo, X., unpublished results.

Chart 1



lifetimes of seven of these styrenes have been measured over a wide range of temperatures and their C=C torsional activation parameters determined by nonlinear fitting of these data using eq 1. The activation parameters are found to be essentially independent of methylation on the C=C bond, but dependent upon the phenyl–vinyl dihedral angle. Styrene and its planar derivatives have C=C torsional barriers of ca. 7 ± 1 kcal/mol, which suffice to inhibit torsion at room temperature. The planar styrenes decay predominantly via fluorescence and intersystem crossing. Styrenes with phenyl–vinyl dihedral angles of ca. $30\text{--}50^\circ$ have torsional barriers of $4\text{--}5$ kcal/mol, which permit singlet state torsion to compete with fluorescence and intersystem crossing. Finally, styrenes with phenyl–vinyl dihedral angles $>60^\circ$ have small apparent barriers, which are attributed to weakly activated intersystem crossing rather than C=C torsion. This unexpected behavior is attributed to breaking conjugation, which results in enhanced spin–orbit coupling in the highly nonplanar styrenes. This model for styrene singlet state decay can also account for the singlet state behavior of two families of cyclic styrene derivatives, the benzocycloalkadienes **10–13**¹² and 1-phenylcycloalkenes **14–16**,¹³ and that of the anti-rotamers of the 2-vinylbiphenyls **17** and **18**.¹⁰

Results

Absorption Spectra. The absorption spectra of **1–5** and **7–11** in methylcyclohexane (MC) solution are shown in Figure 1 and absorption data for styrenes **1–11** summarized in Table 1. The absorption spectra of styrenes **1**, **4**, **10**, and **11** display a weak long-wavelength band with vibronic structure and a

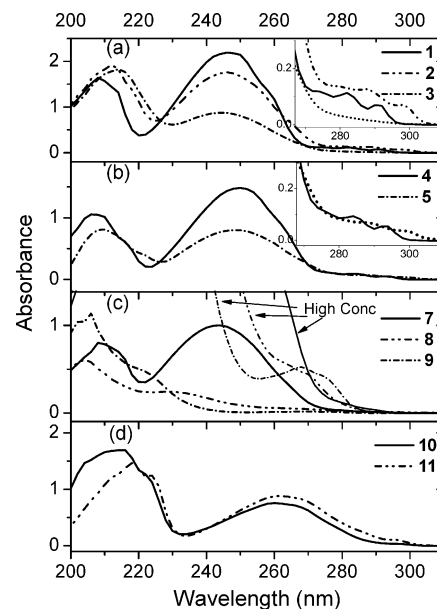


Figure 1. Absorption spectra of styrenes **1–5** and **7–11**.

Table 1. Absorption and Emission Maxima and 0,0 Transitions for Styrenes at Room Temperature

styrene	λ_{amax}^a nm	λ_{lmax}^a nm	0–0 band ^b 10^4 cm^{-1}	Stokes shift ^c cm^{-1}
1	246, (282,292)	304, (293,316)	3.48, 3.48 ^d	2570
2	246, (288, 298)	312, (301, 324)	3.38	2670
3	244	316, (304, 331)	3.33	1,700
4	250, (284,294)	307, (296, 318)	3.45, 3.46 ^d	2640
5	248, (290, 300)	313, (302, 332)	3.38	2530
6	256, (288)	306		
7	244	304, (316)	3.51 ^d	2160
8	230, (282)	311 ^f	3.55 ^g	
9	222, (278)	300 ^f	3.58 ^g	
11	262, (268, 298)	312, (301,324)	3.42	1510
12	260, (266, 298)	312, (301, 325)	3.42	1510

^a Absorption and fluorescence maxima in methylcyclohexane solution at 298 K, except as noted. Shoulders in parentheses. ^b 0,0 transition estimated from excitation and emission spectra. ^c Stokes shift estimated from fluorescence maxima and absorption S_1 shoulder. ^d Data from ref 16. ^f Data obtained at 80 K. ^g Estimated value.

stronger, structureless band at shorter wavelengths. Introduction of an α -methyl substituent (**7**), a 2-methyl substituent (**2** and **5**), or 2,6-dimethyl substituents (**3**) results in loss of vibrational structure in the long-wavelength band and loss of intensity in the short-wavelength band. Styrenes that possess both α - and 2-methyl substituents (**8** and **9**) have red-shifted long-wavelength bands and weak, blue-shifted short-wavelength bands.

To obtain further information about the effects of substituents on the electronic structure and absorption spectra of styrenes, we have performed ZINDO calculations for styrenes **1**, **7**, and **9** using MM/PM3 minimized ground-state geometries.¹⁴ The frontier orbitals involved in the lowest four transitions are depicted graphically in Figure 2, and the calculated energies and oscillator strengths and principal configurations for the lowest four singlet transitions are listed in Table 2. The frontier orbitals of **1** and **7** are delocalized over the entire molecule, except for HOMO-1 and LUMO+1, which are benzene-localized. In contrast, the frontier orbitals of **9** are benzene- or ethylene-localized. The S_1 states of all three styrenes possess a

(11) For a preliminary report see: Lewis, F. D.; Zuo, X. *J. Am. Chem. Soc.* **2003**, *125*, 2046–2047.

(12) Lyons, A. L.; Turro, N. J. *J. Am. Chem. Soc.* **1978**, *100*, 3177–3181.

(13) Zimmerman, H. E.; Kamm, K. S.; Werthemann, D. P. *J. Am. Chem. Soc.* **1975**, *97*, 3718–3725.

(14) *CAChe Release 4.4 Reference*, Version 4.4; Oxford Molecular Group, Inc.: Campbell, CA 95008.

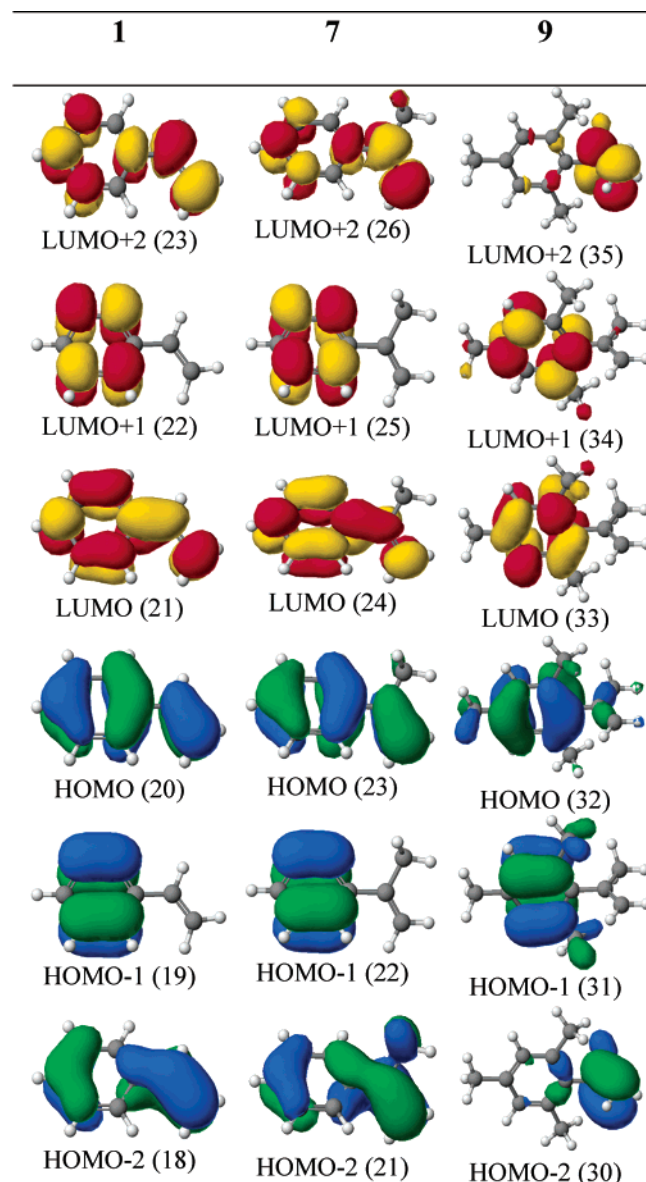


Figure 2. ZINDO Frontier Orbitals for Styrenes 1, 7, and 9.

low oscillator strength and have significant contributions from two or more configurations. The S_2 state of styrene is assigned to an allowed, HOMO–LUMO transition, which is less allowed for 7 and absent in the case of 9.

Fluorescence Spectra. The fluorescence excitation and emission spectra of 1, 7, and 9 are shown in Figure 3. The fluorescence maxima, positions of the 0,0 transitions, and Stokes shifts for 1–11 are reported in Table 1. The 298 K spectra of 2–5 are similar in appearance to that of 1, with excitation spectra displaying a resolved long-wavelength excitation band and emission spectra displaying weak vibronic structure. This long-wavelength excitation band appears as a poorly resolved shoulder in the fluorescence excitation spectra of 7, 8, 10, and 11, which have structureless emission spectra. No room-temperature fluorescence is observed for 9, which displays structureless fluorescence at 80 K.

The fluorescence decay profiles of 1, 2, 7–9, and 11 were measured over extended temperature ranges.¹⁵ The decays at

(15) See Supporting Information.

Table 2. ZINDO Calculations for the Electronic Transitions of Styrenes 1, 7, and 9^a

styrene	transition	energy, nm	f , au ^b	description ^c
1	S ₁	273	0.003	0.62[19,21] – 0.73[20,22]
	S ₂	257	0.41	0.94[20,21]
	S ₃	214	0.47	0.40[19,21] – 0.69[19,21] + 0.36[20,22] – 0.37[20,23]
	S ₄	210	0.79	–0.61[19,21] – 0.49[19,22] + 0.53[20,22]
7	S ₁	270	0.004	0.62[22,24] + 0.72[23,25]
	S ₂	250	0.29	0.32[22,25] – 0.92[23,24]
	S ₃	214	0.29	–0.28[21,24] – 0.74[22,25] – 0.28[23,24] + 0.36[23,26]
	S ₄	208	0.67	–0.66[22,24] – 0.33[22,25] + 0.60[23,25]
9	S ₁	288	0.01	–0.33[31,33] + 0.54[31,34] – 0.67[32,33] + 0.29[32,34]
	S ₂	237	0.10	–0.42[31,33] + 0.46[32,33] – 0.73[32,34]
	S ₃	234	0.00	0.98[32,35]
	S ₄	212	0.68	0.30[30,34] – 0.65[31,34] – 0.49[32,33]

^a ZINDO calculations based on MM/PM3 geometries. ^b f = oscillator strength. ^c Only transitions with coefficients larger than 0.30 are reported.

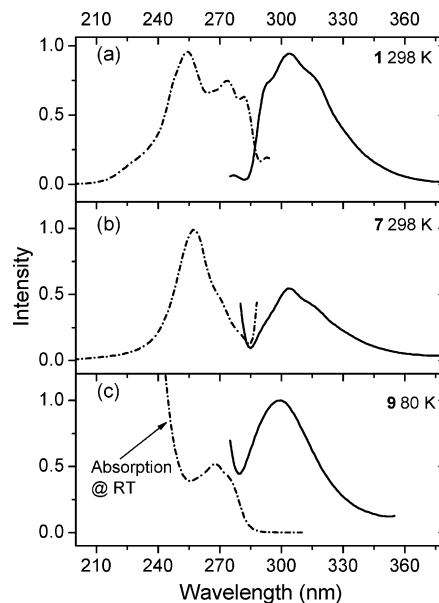


Figure 3. Fluorescence excitation and emission spectra of styrenes 1 and 7 at 298 K and 9 at 80 K.

all temperatures are best fit by a single exponential. Plots of τ_s vs T for 1, 4–9, and 11 are shown in Figure 4 and lifetime data reported in the Supporting Information. The decay times (τ_s) at or near 77 and 298 K are reported in Table 3 along with the fluorescence quantum yields measured at or near 298 K. Also reported in Table 3 are the reported quantum yields and decay times for the cyclic phenylalkenes 12–16.^{12,13}

Ground-State Geometry. Optimized ground-state geometries for 1–16 were calculated using three methods, semiempirical AM1, HF/6-31G^{**}, and DFT-B3LYP/6-31G^{*}. The minimized phenyl–vinyl dihedral angles are reported as Supporting Information along with literature values for some of the styrenes, which have been estimated from spectroscopic studies in jet expansions¹⁶ and from correlations of calculated dihedral angles with absorption maxima.¹⁷ Values of ϕ , the ground-state

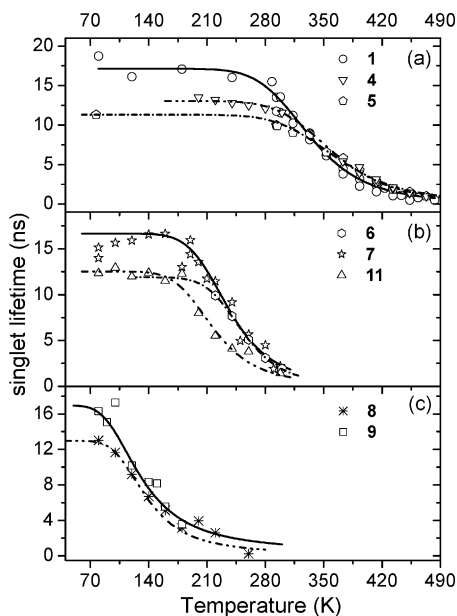


Figure 4. Temperature-dependent lifetimes for styrenes **1**, **4**–**9**, and **11**.

Table 3. Styrene Fluorescence Quantum Yields, Singlet Lifetimes, and Fluorescence Rate Constants^a

styrene	ϕ^b	Φ_f	τ_s , ns (298 K)	τ_s , ns (77 K)	$10^{-7}k_f$, s ⁻¹
1	0	0.24 ^c , 0.22 ^d	13.5, 14.6 ^c , 13.9 ^d	18.7, 18.8 ^c	1.8
2	20	0.19	12.0	11.9	1.6
3	55	0.034	9.5	20.1	0.46
4	0	0.35 ^e	11.3, 11.8 ^e		3.0
5	20	0.33	10.0	11.3	3.3
6	35	0.030, ^d 0.0045 ^e	2.6 ^e , 2.7 ^f		1.2
7	35	0.008, 0.028 ^d	1.5, 2.7 ^d	15.2 ^g	0.55
8	80	0.013		12.4 ^g	
9	90	^h	^h	18.1 ^g	
10	15	0.07, 0.083 ^d	16.1 ^d	18.6	0.50
11	30	0.022	1.2	12.3	1.8
12	20	0.120 ^d	24.2 ^d		0.50
13	60	0.003 ^d	^h		
14	20	0.43 ⁱ	14.3 ⁱ	17.4	3.1
15	45	0.03 ⁱ	1.5 ⁱ	15.8	2.1
16	55	0.016 ⁱ	0.5 ⁱ	9.3	5.7

^a Data in deoxygenated methylcyclohexane solution, 270 nm excitation. Data from this study except as noted. ^b Dihedral angle, see text and Supporting Information. ^c Data from ref 2, used as a secondary fluorescence quantum yield standard, excitation wavelength 250 nm. ^d Data from ref 12, excitation at 260 nm in cyclohexane. ^e Data from ref 7, excitation at 281 nm, in hexanes. ^f Data from ref 1b. ^g Data for 80 K glass. ^h Fluorescence too weak to measure. ⁱ Data from ref 13.

phenyl–vinyl dihedral angle estimated from our calculated values and literature information, are reported in Table 3. The potential energy surfaces for styrenes **1** and **9** calculated at the at HF/6-31G** level are shown in Figure 5. The calculated internal rotational barrier for styrene is 2.9 kcal/mol (4.4 kcal/mol with DFT calculations), consistent with previous experimental results: 3.27 (from single vibronic level fluorescence spectra),¹⁸ 3.09 (from single vibronic level fluorescence and Raman spectra),¹⁹ and 3.29 kcal/mol (from microwave spectroscopy).²⁰

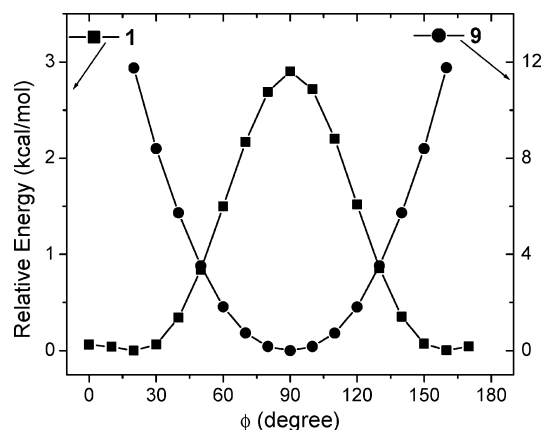


Figure 5. Potential energy surfaces for phenyl–vinyl torsion in styrenes **1** and **9**.

Discussion

Absorption Spectra and Ground-State Geometry. The two lowest energy absorption bands of styrene have been assigned by analogy to the two lowest bands in benzene as arising from a forbidden ¹L_b (¹B₂ ← ¹A₁ in C_{2v} symmetry) transition and an allowed ¹L_a (¹A₁ ← ¹A₁ in C_{2v}, symmetry) transition.^{21,22} With respect to benzene, the styrene transitions are at longer wavelength and closer in energy, as would be expected for a larger p system. Introduction of α -methyl and *ortho*-methyl substituents results in a blue shift in the ¹L_a transition and loss in intensity. This trend has previously been observed by others and attributed to a decrease in molecular planarity as a consequence of nonbonded interactions.^{17,21,23}

Suzuki found that the observed ¹L_a absorption maximum could be correlated with the calculated phenyl–vinyl dihedral angle, ϕ , for a series of alkylated styrenes having values of $\phi < 55^\circ$.¹⁷ A similar correlation including our data for the highly nonplanar styrenes **8** and **9** is shown in Figure 6. These data can be fit to a straight line, even though the ZINDO calculations (Table 2) indicate a change in the character of the lowest energy allowed transition for highly twisted **9** versus planar **1** or moderately twisted **7**. Also shown in Figure 6 are plots of λ_{\max} vs ϕ for the benzocycloalkadienes **10**–**13** and 1-phenylcycloalkenes **14**–**16**. Linear fits of the data for the three families of styrene derivatives (excluding the data for **13**) provide lines of similar slope.

Deviations from the linear correlation in Figure 6 may result from uncertainty in the values of ϕ , which arises from the shallow rotational potentials for most of the styrenes, as illustrated for styrene **1** in Figure 5. Even the highly nonplanar **8** and **9** have shallow potentials in the region of the calculated minimum. AM1 calculations cannot distinguish between the energies of planar and slightly twisted styrenes **1** and **5**. Compared to HF/6-31G** calculations, DFT-B3LYP/6-31G* calculations generally yield more planar structures. As pointed out by Sancho-

(16) (a) Seeman, J. I.; Grassian, V. H.; Bernstein, E. R. *J. Am. Chem. Soc.* **1988**, *110*, 8542–8543. (b) Grassian, V. H.; Bernstein, E. R.; Secor, H. V.; Seeman, J. I. *J. Phys. Chem.* **1989**, *93*, 3470–3474. (c) Grassian, V. H.; Bernstein, E. R.; Secor, H. V.; Seeman, J. I. *J. Phys. Chem.* **1990**, *94*, 6691–6695.
 (17) Suzuki, H. *Electronic Absorption Spectra and Geometry of Organic Molecules*; Academic Press: New York, 1967.

(18) Hollas, J. M.; Ridley, T. *Chem. Phys. Lett.* **1980**, *75*, 94.
 (19) Hollas, J. M.; Musa, H.; Ridley, T.; Turner, P. H.; Weisenberger, K. H.; Fawcett, V. J. *J. Mol. Spectrosc.* **1982**, *94*, 437.
 (20) Caminati, W.; Vogelsanger, B.; Bauder, A. *J. Mol. Spectrosc.* **1988**, *128*, 384.
 (21) Fueno, T.; Yamaguchi, K.; Naka, Y. *Bull. Chem. Soc. Jp.* **1972**, *45*, 3294–3300.
 (22) Michl, J.; Bonačić-Koutecký, V. *Electronic Aspects of Organic Photochemistry*; Wiley-Interscience: New York, 1990.
 (23) Kobayashi, T.; Arai, T.; Sakuragi, H.; Tokumaru, K.; Utsunomiya, C. *Bull. Chem. Soc. Jp.* **1981**, *54*, 1658–1661.

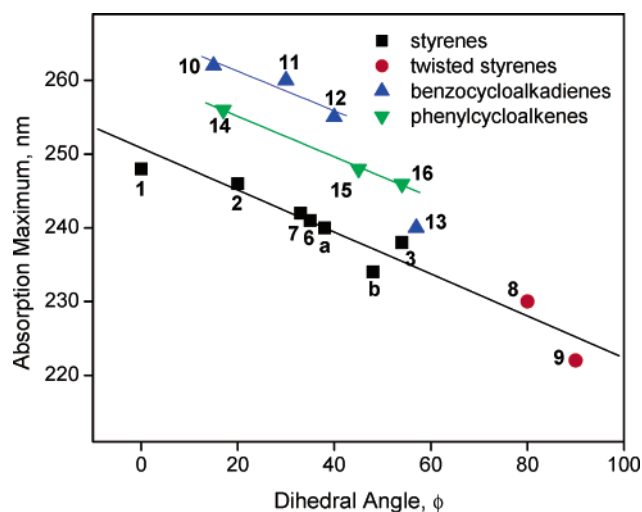


Figure 6. Correlation of the allowed absorption maximum with the phenyl–vinyl dihedral angle for styrenes (**a** = α -ethylstyrene, **b** = α -isopropylstyrene), benzocycloalkadienes, and phenylcycloalkenes. See Chart 1 for structures.

García et al.,²⁴ DFT calculations place a higher weight on conjugation than steric effects.

The relation between planarity and the $S_1 \leftarrow S_0$ transition is more complex. A loss in vibronic structure and resolution of the $S_1 \leftarrow S_0$ and $S_2 \leftarrow S_0$ transitions is observed for styrenes with intermediate twist angles (20° – 40°). However, the $S_1 \leftarrow S_0$ transition is well-resolved for the highly nonplanar styrene **9** (Figure 1).

Fluorescence Spectra and Excited-State Geometry. The fluorescence spectra of the planar styrenes **1**, **2**, **4**, and **5** display weak vibronic structure (Figure 3a) and relatively small Stokes shifts. The moderately nonplanar styrenes such as **3**, **6**, and **7** do not have resolved $S_1 \leftarrow S_0$ transitions in their absorption or excitation spectra, and thus it is not possible to determine their Stokes shifts. Seeman and co-workers¹⁶ found that the S_1 0,0 transition of **7** is blue-shifted 480 cm^{-1} with respect to that of styrene. They also determined that **7** adopts a planar geometry in S_1 , even though it has a value of $\phi \approx 30^\circ$ in S_0 . This behavior can be explained with reference to the characteristics of the S_1 states of styrene (Table 2). S_1 can be described as a combination of (HOMO-1) \rightarrow LUMO and HOMO \rightarrow (LUMO+1) transitions. This shortens the C–C bond by increasing its double bond character.⁵ The enhanced C–C bond order makes the benzene ring and ethylenic group coplanar.

The positions of 0,0 bands in the absorption and fluorescence spectra of styrene are essentially the same (Table 1), in accord with similar planar structures in S_0 and S_1 . Modest Stokes shifts are observed for all of the planar styrenes. In the case of the nonplanar styrenes, the Stokes shifts cannot be estimated due to the absence of a resolved 0,0 absorption band and room-temperature fluorescence. The fluorescence rate constants for the planar styrenes **1** and **2** are $1.7 \pm 0.1 \times 10^7\text{ s}^{-1}$. Somewhat larger values of k_f are observed for the planar β -methyl styrenes **4** and **5**, and a smaller value of k_f is observed for the nonplanar α -methyl styrene **7** (Table 3). These trends roughly parallel the relative intensities of the $S_1 \leftarrow S_0$ transitions (Figure 1).

Table 4. Styrene Activation Parameters and 298 K Rate Constants

styrene	$10^{-7}\Sigma k,^a\text{ s}^{-1}$	$\log A^b$	$E_a,^b\text{ kcal/mol}$	$10^{-7}k_i,^c\text{ s}^{-1}$	$10^{-7}k_{isc},^d\text{ s}^{-1}$
1	5.8 ± 1.3	12.1 ± 0.3	6.6 ± 0.5	1.8	4.0
4	7.7 ± 0.1	12.2 ± 0.2	7.2 ± 0.4	0.89	4.6
5	8.8 ± 0.0	12.0 ± 0.3	6.8 ± 0.5	0.93	4.1
6	8.4 ± 0.1	12.6 ± 0.1	5.4 ± 0.1	4.1	4.6
7	5.7 ± 1.4	11.6 ± 0.9	4.2 ± 1.2	35	5.2
8	7.7 ± 0.4	10.3 ± 0.5	1.6 ± 0.3		150^e
9	5.9 ± 0.5	9.7 ± 0.6	1.4 ± 0.4		86^e
11	8.0 ± 0.2	12.2 ± 0.8	4.3 ± 0.8	130	6.2

^a Sum of the nonactivated singlet decay processes at 298 K. ^b Activation parameters for singlet activated decay from nonlinear fitting of temperature-dependent lifetimes (Figure 4). ^c Room temperature double bond twisting rate k_i calculated from A and E_a . ^d Intersystem crossing rate constant $k_{isc} = \Sigma k - k_f$ (values of k_f from Table 3), excepted as noted. ^e Calculated from measured activation parameters.

Nonradiative Decay of Planar Singlet States. Our earlier study of the photochemical behavior of the singlet state of *trans*- and *cis*-1-phenylpropene (**4** and **6**) established the existence of two nonradiative pathways, intersystem crossing and *trans,cis* isomerization.^{6,7} Internal conversion of the planar singlet evidently does not compete with these processes.⁷ Measurement of the isomerization quantum yield and singlet lifetime over a broad temperature range provided the temperature-dependent rate constants for isomerization calculated using eq 2, where the factor of 2 reflects the partitioning of the twisted intermediate between *cis* and *trans* ground states. The curved Arrhenius plots were analyzed to provide rate constants for intersystem crossing and the activation parameters for singlet state isomerization using eq 3, which requires the assumption that k_{isc} is unactivated. Reanalysis of the lifetime data using eq 1 provides values of Σk , the sum of the unactivated rate constants, and the activation parameters for activated nonradiative decay. The latter are in good agreement with those obtained from eq 3. Thus we conclude that **4** and **6** undergo a single activated nonradiative decay process, namely torsion about the C=C double bond (Chart 1, θ)

$$k_{iso}(T) = 2 \times \frac{\Phi_{iso}(T)}{\tau(T)} \quad (2)$$

$$k_{iso}(T) = k_{isc} + Ae^{(-E_a/RT)} \quad (3)$$

Nonlinear fits of the temperature-dependent lifetime data for styrenes **1**, **4**–**9**, and **11** to eq 1 are shown in Figure 4 and the resulting values of Σk , $\log A$ and E_a reported in Table 4. This analysis requires the assumption that neither k_f nor k_{isc} is temperature dependent, in accord with the results of our studies of **4**⁷ and 1,3-diphenylpropenes.⁸ The values of $\log A$ and E_a are similar for the planar styrenes **1**, **4**, and **5**. The moderately nonplanar styrenes **6** and **7** and α -methyl-dihydronaphthalene, **11**, have values of $\log A$ similar to those of the planar styrenes and somewhat smaller values of E_a . Values of $\log A \approx 12$ are consistent with a unimolecular isomerization reaction. Thus, we conclude that the activated nonradiative decay channel for all of the planar styrenes (**1**, **4**, and **5**) and moderately nonplanar styrenes (**6** and **7**) is C=C torsion.

The C=C torsional barrier in styrene has been attributed to the avoided crossing between the planar S_1 state and an upper singlet state (S_n) which correlates with the twisted singlet state

(24) Sancho-García, J. C.; Pérez-Jiménez, A. J. *J. Phys. B: At. Mol. Opt. Phys.* **2002**, *35*, 1509–1523.

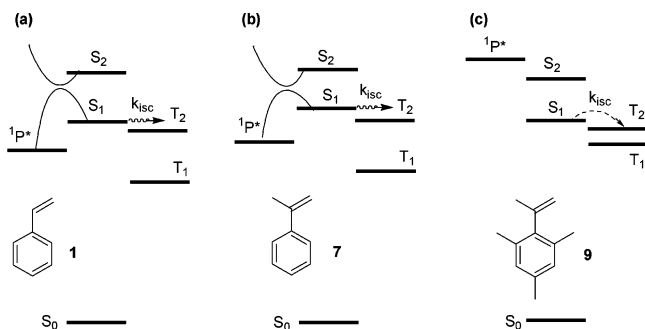


Figure 7. Approximate state energy diagrams for styrenes **1** (a), **7** (b), and **9** (c). See text for description of state energies.

$^1P^*$ (Figure 7a).³ The decreased barrier for **6** and **7** may reflect increased nonbonded repulsion in their planar S_1 states, which could lower the barrier for C=C torsion (Figure 7b). As a consequence of the large torsional barrier, the planar styrenes decay largely via fluorescence and intersystem crossing at room temperature. The lower torsional barriers for **6** and **7** permit singlet state torsion to compete more effectively with fluorescence and intersystem crossing. Interestingly, β -methyl substituents do not lower the torsional barrier, even though they might be expected to stabilize the $^1P^*$ state. We previously observed that solvent polarity and aromatic substituents also have only minor effects on the torsional barrier for **4**.⁷

Rate constants for intersystem crossing for the planar and moderately nonplanar styrenes can be calculated from the values of Σk obtained from nonlinear fitting (Table 4) and the fluorescence rate constants determined from the lifetime and quantum yield (Table 3), assuming that the planar singlets do not undergo internal conversion.⁷ Values of $k_{isc} \approx 5 \times 10^7 \text{ s}^{-1}$ are obtained in this fashion for **1** and **4–7**. Ni et al.²⁵ report a vertical triplet energy of 60.5 kcal for **4**, approximately 36 kcal lower than the S_1 0,0 energy. A much smaller value of k_{isc} would be expected for a $^3\pi,\pi^* \leftarrow ^1\pi,\pi^*$ intersystem crossing process with such a large energy gap.²⁶ Thus, we conclude that intersystem crossing involves an upper triplet, presumably T_2 (Figure 7a), as is the case for anthracene. Bearpark et al.³ have in fact predicted that S_1/T_2 intersystem crossing is the temperature-independent nonradiative decay pathway for styrene. The similar values of k_{isc} and k_f for the planar and moderately nonplanar styrenes is indicative of similar excited-state geometries, as found by Seeman and co-workers¹⁶ in their studies of the S_1 geometries of **1** and **7**.

Nonradiative Decay of Nonplanar Singlet States. Nonlinear fitting of the temperature-dependent lifetimes of the nonplanar styrenes using eq 1, **8** and **9** provides values of $\log A \approx 10$ and $E_a \approx 1.5 \text{ kcal/mol}$. The low barrier might be simply interpreted as a continuation of the trend observed for styrenes **6** and **7**. However, the large S_1 – S_2 energy gap for **9**, which is apparent both in the absorption spectrum (Figure 1) and the ZINDO calculations (Table 2), is inconsistent with a low C=C torsional barrier. Furthermore, due to the large phenyl–vinyl dihedral angle, the $^1P^*$ state should lie well above the benzene-localized lowest excited singlet states. Michl and Bonačić-Koutecký calculate a $^1P^*$ energy of $\sim 130 \text{ kcal/mol}$ for ethylene.²² In

addition, the values of $\log A$ are much smaller than those for the planar styrenes and would be exceptionally small for a singlet state isomerization processes. Imposing a higher value of $\log A$ upon the data worsens the fit for E_a . These factors argue for a change in mechanism for the nonradiative singlet decay of the highly twisted styrenes **8** and **9**.

The low values of $\log A$ and E_a suggest the possibility of weakly activated intersystem crossing from the benzene-localized $^1\pi,\pi^*$ state to the ethylene-localized $^3\pi,\pi^*$ state as the predominant pathway for decay of singlet **8** and **9**. Ni et al.²⁵ report similar triplet energies for the spectroscopic triplet states of benzene and ethylene (ca. 84 kcal/mol), however, the relaxed triplet of ethylene should be at lower energy than that of benzene. $^3\pi,\pi^* \leftarrow ^1\pi,\pi^*$ intersystem crossing is generally slow in planar aromatic molecules, including styrene.²⁶ However, the twisted geometry of **8** or **9** provides the orthogonal relationship between the benzene and vinyl π -orbitals necessary for effective spin–orbit coupling between the benzene-localized S_1 state and the ethylene-localized triplet state.^{26,27}

A tentative state energy diagram for **9** is shown in Figure 7c. According to this diagram, the 298 K rate constant calculated from the activation parameters for **8** and **9** is assigned to k_{isc} . The calculated values of k_{isc} are substantially faster than those for the planar styrenes (Table 4). However, they are slower than the value of $k_{isc} = 4 \times 10^{10} \text{ s}^{-1}$ for acetophenone $^3\pi,\pi^* \leftarrow ^1n,\pi^*$ intersystem crossing.²⁸ This difference can be attributed to the location of the orthogonal π -orbitals of **8** or **9** on adjacent atoms, rather than on the same atom, as in acetophenone.^{22,26} Out-of-plane vibrations are known to serve as promoting modes for $^1\pi,\pi^* \rightarrow ^3\pi,\pi^*$ intersystem crossing.²⁹ Thus, the activated nature of the singlet decay of **8** and **9**, (Table 4), may reflect the solvent-viscosity dependence of these vibronic interactions.

Summary

According to our model for the behavior of the styrene singlet state (Figure 7), the activated nonradiative decay process depends on the ground-state phenyl–vinyl dihedral angle, ϕ . Styrenes with small values of ϕ ($< 30^\circ$) are expected to have large barriers for C=C torsion ($> 6 \text{ kcal/mol}$), slow intersystem crossing rate constants, and long 298 K singlet lifetimes. Styrenes with intermediate values of ϕ (30 – 60°) are expected to have smaller barriers for C=C torsion (4 – 6 kcal/mol) and short 298 K singlet lifetimes. Styrenes with large values of ($\phi > 60^\circ$) are expected to undergo weakly activated intersystem crossing and have very short 298 K singlet lifetimes. The dependence of E_a and τ_s on ϕ is shown in Figure 8 for the styrenes in Table 4. A gradual decrease in E_a with increasing ϕ is observed for values of $\phi < 60^\circ$ with an abrupt decrease for $\phi > 60^\circ$. This decrease is attributed to breaking of styrene conjugation which results in enhanced spin–orbit coupling. The 298 K values of τ_s drop abruptly for values of $\phi > 30^\circ$ as a consequence of a rather modest change in the value of E_a for C=C torsion. Thus the 298 K singlet lifetimes by themselves do not serve to distinguish between the behavior of moderately and highly twisted styrenes.

(25) Ni, T.; Caldwell, R. A.; Melton, L. A. *J. Am. Chem. Soc.* **1989**, *111*, 457–464.

(26) Turro, N. J. *Modern Molecular Photochemistry*; Benjamin/Cummings: Menlo Park, CA, 1978.

(27) Klessinger, M.; Michl, J. *Excited States and Photochemistry of Organic Molecules*; VCH Publishers: New York, 1995.

(28) McGarry, P. F.; Doubleday, C. E., Jr.; Wu, C.-H.; Staab, H. A.; Turro, N. J. *J. Photochem. Photobiol. A: Chem.* **1994**, *77*, 109–117.

(29) Lim, E. C. In *Excited States*; Lim, E. C., Ed.; Academic Press: New York, 1977; Vol. 3, pp 305–337.

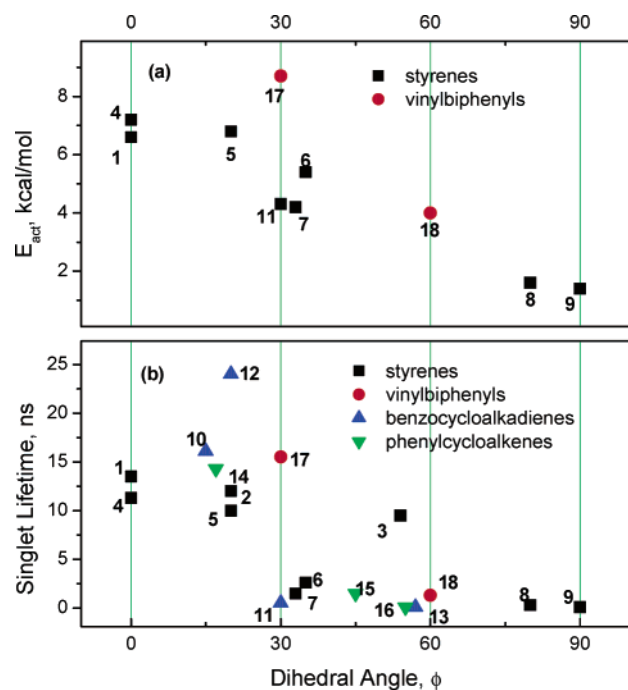


Figure 8. Phenyl–vinyl dihedral angle dependence of (a) the activation energies for C=C torsion and (b) the singlet lifetimes of some styrenes and vinylbiphenyls.

Related Systems. We have recently determined the torsional barriers for the anti-rotamers of 2-vinylbiphenyl (**17**) and 2-(2-propenyl)biphenyl (**18**), which have ground-state phenyl–vinyl dihedral angles of ca. 30° and 60°, respectively.¹⁰ They both have values of $\log A \approx 12.5 \pm 0.5$ and values of $E_a = 8.7$ and 4.4 kcal/mol, respectively. Their activation energies and 298 K lifetimes are included in Figure 8 and are compatible with the styrene data. Also included in Figure 8b are the 298 K lifetimes of the benzocycloalkadienes **10–13**, and the phenylcycloalkenes **14–16**. Lyons and Turro¹² reported that the benzocycloalkadienes **10** and **12** have moderately long lifetimes (> 15 ns) and values of $\Phi_f \approx 0.1$ at room temperature (Table 3), indicative of large torsional barriers. In contrast, **13** has a short singlet lifetime and very low Φ_f , indicative of a relatively small torsional barrier or fast intersystem crossing. They attributed the difference in lifetimes to inhibited C=C torsion in the smaller rings. However, as we have shown, acyclic planar styrenes such as **1** and **4** also have large barriers for C=C torsion. Thus, we attribute the short singlet lifetime of **13** to a large phenyl–vinyl dihedral (ca. 60°, Table 3). The introduction of a 1-methyl substituent in **11** results in a dihedral angle similar to that of **13** and a measured barrier for singlet state C=C torsion of 4.3 kcal/mol (Table 4). A barrier of similar magnitude could account for the short singlet lifetime of **13**. Zimmerman, Kamm, and Werthemann¹³ reported that the singlet lifetimes of **14–16** decrease with increasing ring size (Table 3). This trend was also attributed to inhibited C=C torsion in smaller rings. However, their lifetime data can also be correlated with the phenyl–vinyl dihedral angle (Figure 8b), the planar **14** having the largest C=C torsional barrier and **16** having the largest dihedral angle and shortest singlet lifetime. We also think it unlikely that the phenylcycloalkenes **14–16** undergo singlet internal conversion, as previously suggested,¹³ and attribute their

low-temperature nonradiative decay to intersystem crossing rather than internal conversion.

Experimental Section

General Methods. ¹H NMR spectra were measured on a Varian Gemini 400 spectrometer. GLC analysis was performed on a Hewlett-Packard HP 5890 instrument equipped with a HP poly(dimethylsiloxane) capillary column. UV–vis spectra were measured on a Hewlett-Packard 8452A diode array spectrometer with a 1 cm path length quartz cell. Fluorescence spectra were measured on a SPEX Fluoromax spectrometer. *trans*- β -Methylstyrene or styrene ($\Phi_f = 0.36^7$ or 0.24^2 in hexanes, respectively) was used as a secondary standard for the measurement of fluorescence quantum yields. Fluorescence quantum yields were measured by comparing the integrated area under the fluorescence curve to that of the secondary standard at equal absorbance (ca. 0.1 OD) at the same excitation wavelength. All fluorescence spectra are uncorrected, and the estimated error for the fluorescence quantum yields is $\pm 10\%$. Fluorescence decays were measured on a Photon Technologies International LS-1 single photon counting apparatus with a gated hydrogen arc lamp using a scatter solution to profile the instrument response function. Nonlinear least-squares fitting of the decay curves were performed with the Levenburg–Marquardt algorithm as described by James et al.³⁰ and implemented by the Photon Technologies International Timemaster (version 1.2) software. Goodness of fit was determined by judging the χ^2 (< 1.3 in all cases), the residuals, and the Durbin–Watson parameter (> 1.6 in all cases).

For temperatures below ambient, a nitrogen-cooled Oxford Instruments optical cryostat (DN 1704) and ITC temperature controller were used to maintain the sample temperature within ± 0.1 K of the desired value. For temperature above ambient, a circulating water–ethylene glycol bath was used to control the sample temperature ± 0.2 K of the desired value, up to 80 °C. A homemade high-temperature high-pressure stainless steel cell and ITC temperature controller were used for a wider temperature range, from room temperature to 200 °C. At each temperature, a time period of 30 min was needed to allow the sample to reach temperature equilibrium.

INDO/S-CIS-SCF (ZINDO) calculations (26 occupied and 26 unoccupied frontier orbitals) were performed on a PC with the ZINDO Hamiltonian as implemented by CAChe Release 4.4.¹⁴ Optimized ground-state geometries used in the semiempirical calculations were obtained from MM/PM3 calculations using the MOPAC suite of programs in Chem Office 6.0. Potential energy surfaces were calculated using Jaguar with closed-shell restricted Hartree–Fock type.³¹ All data fitting procedures were carried out by using Origin (version 6.1).³²

Materials. Styrenes **1–4** and **7–10** were obtained from commercial sources. Styrenes **5** and **11** were prepared by the methods of Adamczyk et al.³³ and Wehrli et al.,³⁴ respectively, purified by column chromatograph and characterized spectroscopically. All styrenes were of >99% purity by GC analysis.

(30) James, D. R.; Siemiarz, A.; Ware, W. R. *Rev. Sci. Instrum.* **1992**, *63*, 1710.

(31) *Jaguar 4.1 Release 45 reference*, Version 4.1 Release 45; Schrödinger, Inc.: Portland, OR 97201.

(32) Origin Version 6.1; Microcal Software, Inc.: Northampton, MA, 2000.

(33) Adamczyk, M.; Watt, D. S.; Netzel, D. A. *J. Org. Chem.* **1984**, *49*, 4226–4237.

(34) Wehrli, R.; Heimgartner, H.; Schmid, H.; J., H. H. *Helv. Chim. Acta* **1977**, *60*, 2034–2061.

Acknowledgment. Funding for this project was provided by NSF Grant No. CHE-0100596.

Supporting Information Available: Tables reporting singlet lifetimes as a function of temperature and the calculated and

literature values of the phenyl–vinyl dihedral angles. This material is available free of charge via the Internet at <http://pubs.acs.org>.

JA035066J